Efficient Modal Design Variables Applied to Aerodynamic Optimization of a Modern Transport Wing

C.B. Allen *, D.J. Poole †, T.C.S. Rendall‡

Department of Aerospace Engineering, University of Bristol, Bristol, BS8 1TR, U.K.

Aerodynamic shape optimization of a transonic wing using mathematically-extracted modal design variables is presented. A novel approach is used for deriving design variables using a proper orthogonal decomposition of a set of training aerofoils to obtain an efficient, reduced set of deformation 'modes' that represent typical design parameters. A major advantage of this extraction method is the production of orthogonal design variables, and this is particularly important in aerodynamic shape optimization. These design parameters have been tested previously on geometric shape recovery problems and aerodynamic shape optimization in two dimensions, and been shown to be efficient at covering a large portion of the design space, hence the work is extended here to consider their use in three dimensions. It has been shown previously that fewer than 10 aerofoil modes are required to obtain shock free solutions from initial strong shock, highly-loaded aerofoils. Wing shape optimization in transonic flow is performed here using an upwind flow-solver and parallel gradient-based optimizer, and a small number of global deformation modes are compared to a section-based local application of these modes and to a previously-used section-based domain element approach to surface deformations. The modal approach is shown to be particularly effective, with local application of modal design variables resulting in a shock-free solution and a 30% reduction in drag.

I. Introduction and Background

Numerical simulation methods to model fluid flows are used routinely in industrial design, and increasing computer power has resulted in their integration into aerodynamic shape optimization (ASO) frameworks. The aerodynamic model is used to evaluate some metric against which to optimize, which in the case of ASO is an aerodynamic quantity, most commonly drag, subject to a set of constraints which are usually aerodynamic or geometric. Along with the fluid flow model, the ASO framework requires a surface parameterization scheme, which describes mathematically the aerodynamic shape being optimized by a series of design variables. Changes in the design variables, which are made by a numerical optimization algorithm, result in changes in the aerodynamic surface. Numerous advanced optimizations using compressible computational fluid dynamics (CFD) as the aerodynamic model have been performed previously,[1,2,3,4,5] and the authors have presented work in this area, having developed a modularised, generic optimization tool, that is flow-solver and mesh type independent, and applicable to any aerodynamic problem.[6,7,8]

The fidelity of results obtained by the optimization process are dependent on the fidelity and quality of each of the three individual components of the ASO process; optimization algorithm, shape parameterization and aerodynamic model. To facilitate optimum compatibility between these components, each is often designed in a modular manner such that, for example, the aerodynamic model is independent of the parameterization scheme used. A high fidelity numerical aerodynamic model with good capture of the true physics is important in producing optimum aerodynamic designs, particularly at transonic conditions, and the aerodynamic model also defines the parameter space of the problem, which is the definition of the aerodynamic outputs based on flow field inputs such as Mach number and angle of attack.

*Professor of computational aerodynamics, AIAA Senior Member. Email: c.b.allen@bristol.ac.uk
†Graduate Student. Email: dp8470@bristol.ac.uk
‡Lecturer, Aerospace Engineering Department. Email: thomas.rendall@bristol.ac.uk

The quality of the optimization result obtained is driven, primarily, by the quality and type of numerical optimization algorithm used in the ASO framework, and the two primary types of optimization algorithms are local methods and global methods. Local methods are usually built around the gradient-based approach, which uses the local gradient of the design space as a basis around which to construct a search direction. These approaches are the most common methods used in the ASO framework ([9,10,4] for example), driven primarily by the low cost associated with them compared to global methods.[11] Global optimization algorithms, on the other hand, tend to be based around a swarm intelligence approach, where candidate solutions scattered throughout the design space cooperate together to locate the global optimum solution. These algorithms are much less prone to converging in local optimum solutions that are not necessarily close to the global optimum. However, they are often considerably more expensive than the local algorithms, and handling of constraints can be difficult and is often done on an *ad hoc* basis, and so the use of global optimizers in ASO is more restricted than local methods, although it is becoming more common.[12,13]

The aerodynamic model defines the parameter space of the problem, however the problem design space, which the optimization algorithm interrogates, is constructed by the definition of a surface parameterization scheme. The ability of the optimizer to fully interrogate the true design space (which contains every possible design) is driven by the ability for the degrees of freedom of the parameterization scheme to represent any shape within the design space, and so this is a critical aspect of any optimization scheme. Furthermore, the use of a low number of design variables is generally advantageous, particularly if global optimization algorithms are used where good convergence of these algorithms tends to correlate with small numbers of design variables.

An important aspect of any parameterization scheme is orthogonality of the design variables. Orthogonal design variables means that a shape is represented by a unique set of inputs, often leading to a design space that is more efficient meaning it can be represented with many fewer design variables.[14] It also tends to simplify considerably the design space against non-orthogonal design variables and leads to greater coverage of the design space, i.e. the design variables can represent a greater number of aerodynamic shapes; the design space of N design variables is always contained within the design space of $N + n$ design variables.

The work presented in this paper considers aerodynamic shape optimization using a novel method of deriving design variables. The design variables used here are derived by a mathematical technique that is based on proper orthogonal decomposition (POD), that extracts an orthogonal set of geometric 'modes'. The method itself has been presented recently by the authors,[15] and has been shown to outperform other commonly used parameterization schemes[16] when considering geometric inverse design in two dimensions, often requiring less than a dozen variables to represent a large design space.

The aim of the work presented here is to develop an effective method to apply these novel mathematically-extracted design variables in three dimensions, and determine their effectiveness when applied to aerodynamic optimization, in particular drag minimisation of wings in transonic flow.

I.A. Aerofoil Parameterization and Deformation Approaches

A surface parameterization scheme defines a design space by a number of design variables. A separate problem to this, though often considered alongside, is the deformation of the subsequent surface during the optimization process, which is required to allow deformation of a body-fitted CFD mesh. The effectiveness of a parameterization method is i) being flexible and robust enough to cover the design space, and ii) efficient enough to represent a given shape with as few design variables as possible. Methods are classified as either constructive, deformative or unified. In-depth reviews have been presented by Samareh,[17] Nadarajah *et al.*[14,18] and Masters *et al.*[16]

Constructive methods consider the definition of the surface and the deformation of the surface separately. Examples of these methods are CST,[19] PARSEC,[20] PDEs[21] and splines.[22] Other approaches that combine various parameterizations in a hybrid approach, such as that of Zhu and Qin[23] can also be found. Due to the constructive nature of these approaches, perturbation of the base geometry through the optimization process therefore requires that the new surface be reconstructed, which subsequently requires automatic mesh generation tools for production of a new surface and volume mesh. This extra difficulty can make it advantageous to consider approaches that manipulate an existing mesh.

An alternative to constructive are deformative methods which unify the geometry creation and perturbation. This tends to make them simpler to integrate with mesh deformation tools and allows the use of previously generated meshes; a considerably cheaper alternative to regeneration, although the mesh deformation scheme is a separate algorithm. Analytic[1] and discrete[24] methods are examples of deformative

approaches.

A further refinement of unifying geometry creation and perturbation is the integration with a mesh deformation algorithm. Methods of this type typically have some interpolation that describes a link between the surface and volume, often via a set of control points that are independent of both, such that deformation of the control points results in deformation of the surface and CFD mesh. These approaches are commonly used in ASO, and the methods included in this unified category are free-form deformation[25] (FFD), domain elements[6] and direct manipulation.[26]

A novel method, recently developed by the authors, is to extract aerofoil design variables using a mathematical approach. The approach utilises singular value decomposition (SVD) in a manner that analyses an initial library of aerofoils and decomposes that library into a reduced set of optimum variables that are geometrically orthogonal to each another. The method is independent of the geometry so can fit into either one of the three categories outlined above; the deformative formulation is used in this work. It can also be linked to a unified approach to allow the design variables to be applied to the unified method, which is also the method used in this work to allow application of the parameters to ASO. Previous work has considered the ability for the method to represent a wide-range of aerofoil shapes,[15,27,16,28] and the work here extends the work to application to three-dimensional wing optimization.

I.B. Three-dimensional Aerodynamic Shape Optimization

The optimization of aircraft wings that represent a typical condition of a modern-day airliner at cruise conditions is probably the most common type of three-dimensional aerodynamic shape optimization performed. The initial studies into this type of problem were performed by Jameson *et al.*,[29,30,31] who showed that the adjoint (or control theory) approach for obtaining gradients can lead to high quality optimization results. The adjoint method has the advantage of being able to compute large numbers of design variables in one solution, allowing every surface point to be used as a design variable in the optimization process. However, while large numbers of design variables can be handled by the adjoint method, the design spaces of such problems are likely to be complex and highly multimodal (this has been demonstrated for wing optimization in a comprehensive study by Chernukhin and Zingg[11]) making it difficult for a gradient-based optimization algorithm to make large planform changes and minor surface changes at the same time.

Surface parameterizations developed around the FFD and domain element approach are very popular in wing optimization as this type of approach allows the design space to be reduced from thousands of design parameters to hundreds of design parameters. Such techniques have been developed by Zingg and colleagues,[10,32] and have shown that these type of methods can be flexible enough to allow the moulding of a sphere into an aircraft like shape under certain optimization conditions.[33] Further work has also been performed by Martins *et al.*[34,35] who showed results for blended-wing-body optimizations, and Yamazaki *et al.*[26] who further reduced the number of design variables by considering the direct manipulation method for wing optimization.

Typically, owing to the high cost associated with running high-fidelity simulations in three-dimensions, numbers of objective function evaluations are kept to a minimum hence gradient-based optimization algorithms are often run. With increasing computing power available to researchers, however, global search algorithms are now also being used for wing optimization problems. Global search algorithms have the advantage of not being constrained by restrictions placed on the algorithm by gradient computations such as termination in local minima, hence are generally better at locating globally optimal solutions in multimodal spaces. Examples of such optimizations have been shown for genetic[36] and particle[13] approaches. Whichever optimisation approach is used, the number of design variables required to cover the design space is a very important consideration, and the modal approach used here has been shown to be very efficient.[37]

II. Parameterization Scheme

The modal design variables used here are based on aerofoil surface deformations and are linked to a unified parameterization scheme which uses control points to deform the CFD mesh, which is also called the domain element approach. The method for deriving the mathematical design variables is outlined first, followed by the control point-based approach for deforming the CFD mesh.

II.A. Aerofoil Deformations by Singular Value Decomposition

The derivation of aerofoil perturbation modes come from a proper orthogonal decomposition (POD), via singular value decomposition (SVD) of a training library of aerofoils. The resulting modes, which form aerofoil design variables used in this work for ASO, are guaranteed to be orthogonal, meaning a given aerofoil shape is described uniquely by a given set of input parameters. This alleviates some multimodality that can be introduced numerically by the given parameterization scheme, and expands design space coverage.[14] An alternative to deriving design variables by a direct decomposition approach is to manipulate already existing ones by Gram-Schmidt orthogonalisation. This can be used to force orthogonality,[38,39] however, it is ideal to use the SVD method to guarantee orthogonal modes and provide a low dimensional approximation (modal parameters) to a high dimensional design space (full training library). Initial studies of using the SVD method to derive design variables have previously been demonstrated by Toal *et al.*[40] and Ghoman *et al.*,[41] however, the work presented here develops more fully the use of mathematically-derived modes for performing aerodynamic shape optimization.

The SVD method first requires a training library of N_a aerofoils to be collated from which the aerofoil deformation modes are extracted. Each aerofoil surface is parameterized by N surface points, where the i-th surface point has a position in the space (x_i, z_i). To ensure consistency of the surface description of the training data all aerofoils are parameterized with the same parametric distribution, followed by each aerofoil having a rigid body translation, scaling and then rotation applied to it to map the geometry into a consistent form where the leading edge is located at the origin and the trailing edge at unit chord along the horizontal axis. A matrix is built from which SVD is performed, by evaluating the vector difference of the i-th surface point between all aerofoils, producing $N_{def} = N_a(N_a - 1)/2$ aerofoil deformations. The x and z deformations are stacked into a single vector of length $2N$, for each aerofoil deformation, so a matrix is built of the aerofoil deformations which has $2N$ rows and N_{def} columns:

$$\mathbf{M} = \begin{pmatrix} \Delta x_{1,1} & \cdots & \Delta x_{1,N_{def}} \\ \vdots & \ddots & \vdots \\ \Delta x_{N,1} & \cdots & \Delta x_{N,N_{def}} \\ \Delta z_{1,1} & \cdots & \Delta z_{1,N_{def}} \\ \vdots & \ddots & \vdots \\ \Delta z_{N,1} & \cdots & \Delta z_{N,N_{def}} \end{pmatrix} \tag{1}$$

Performing a SVD decomposes the matrix into three constituent matrices:

$$\mathbf{M} = \mathbf{U}\mathbf{\Sigma}\mathbf{V}^T \tag{2}$$

where $\mathbf{U}$ is a matrix of vectors, each of length $2N$. The structure is analogous to the decomposed matrix, so the columns of this matrix are the aerofoil mode shapes. $\mathbf{\Sigma}$ is a diagonal matrix of the singular values, arranged in descending order. These can be considered the 'relative energy' of the modes, and represent the 'importance' of the mode shapes in the original library. The total number of possible mode shapes is governed by the number of singular values, which is the minimum of the number of columns and rows of the decomposed matrix. A truncation of the $\mathbf{U}$ matrix, based on a certain total energy required, then gives the number of design variables used in the optimization. The training library is based on deformations and this is an important choice such that design variables that result from the decomposition are also deformations, ensuring they are independent of the topology of the aerofoils that are used. This allows direct insertion into an aerodynamic shape optimization framework where deformation of the surface and mesh is important. If the constructive formulation is used, however, then the columns of the training matrix, $\mathbf{M}$, can be absolute positions of the aerofoil surface points as opposed to deformations between surface points.

In this work, a generic, non-symmetric training library is considered based on the optimization being performed. The library contains 100 different aerofoils, extracted from a larger library by quantifying their performances in the transonic regime using the technology factor.[15] The first six modes of the library are shown in figure 1; all modes are scaled up for illustration purposes, and have been added to a NACA0012 section.

Once the design variables have been extracted, and the total number of modes has been truncated then a new aerofoil can be formed by a weighted combination of m modal parameters, as shown in equations 3. The weighting vector, $\boldsymbol{\beta}$, represent the magnitude of the modal deformations which are then the design

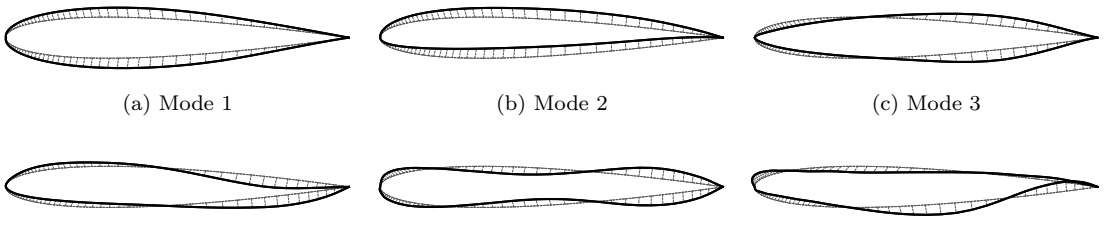

(a) Mode 1 (b) Mode 2 (c) Mode 3

(d) Mode 4 (e) Mode 5 (f) Mode 6

Figure 1: Generic non-symmetric aerofoil modes.

variable values the optimizer works with. The truncation of the total number of modes, which is often very large, down to a number which is useful for the optimization can either be done by a user specified number or based on the requirement for a total amount of energy to be preserved i.e. if 99.0% of the energy of the original library is required to be preserved then the first, say, six modes may cumulatively have 99.1% of the energy so six modes would be used. In this work, a number of modes is specified and those modes with the highest amount of energy are taken.

$$\begin{pmatrix} x_1 \\ \vdots \\ x_N \\ z_1 \\ \vdots \\ z_N \end{pmatrix}^{new} = \begin{pmatrix} x_1 \\ \vdots \\ x_N \\ z_1 \\ \vdots \\ z_N \end{pmatrix}^{old} + \sum_{n=1}^{m} \beta_n \begin{pmatrix} U_1^n \\ \vdots \\ U_N^n \\ U_{N+1}^n \\ \vdots \\ U_{2N}^n \end{pmatrix} \quad \text{or} \quad \mathbf{X}^{new} = \mathbf{X}^{old} + \sum_{n=1}^{m} \beta^n \mathbf{U}^n \tag{3}$$

II.B. RBF Coupling of Point Sets for Aerofoil Deformation

The aerofoil design variables must be coupled to a control-point based approach to allow flexible deformation of the CFD mesh. The control point method links deformations of the CFD mesh to deformations of a small set of control points on or near the surface. At the centre of this technique is a multivariate interpolation using radial basis functions (RBFs), which provides a direct mapping between the control points, the surface geometry and the locations of grid points in the CFD volume mesh. The approach is meshless, so requires no connectivity and is applicable to any mesh type; control points and volume mesh points are simply treated as independent point clouds. The system is only the size of the number of control points, and so is not related to the mesh size.

The general theory of RBFs is presented by Buhmann[42] and Wendland,[43] and the basis of the method used here is described in detail by Rendall and Allen.[44] Let $f(\mathbf{x})$ be the original function to be modelled, and f_i be the scalar values at n discrete points $\mathbf{x}_i, i = 1, ..., n$, where $\mathbf{x}_i$ is the vector of inputs at the ith sample point. The set of data points $\mathcal{X} = \{\mathbf{x}_1, ..., \mathbf{x}_n\}$ is confined to a domain Ω in d-dimensional space. A RBF model is then a linear combination of basis functions, whose argument is the Euclidean distance between the point $\mathbf{x}$ at which the interpolation is made and the n points in the known data set. In other words, the interpolation at an untried site is a sum of contributions from all the known function values, the influence of which is controlled by a basis function that depends on the distance they are from the new site. If ϕ is the chosen basis function and $\|\cdot\|$ is used to denote the Euclidean norm, then an interpolation model s has the form

$$s(\mathbf{x}) = \sum_{i=1}^{n} \alpha_i \phi(\|\mathbf{x} - \mathbf{x}_i\|) + p(\mathbf{x}) \tag{4}$$

where $\alpha_i, i = 1, ..., n$ are model coefficients, and $p(\mathbf{x})$ is an optional polynomial. The coefficients are found by requiring exact recovery of the original data, $\mathbf{s}_\mathcal{X} = \mathbf{f}$, for all points in the training data set $\mathcal{X}$. Hence

the model is an interpolant, and all original solution information is preserved. When the polynomial term is included, the system is completed by the additional requirement

$$\sum_{i=1}^{n} \alpha_i p(\mathbf{x}) = 0 \tag{5}$$

which is sometimes referred to as the side condition, for a polynomial that takes the form

$$p^x = \gamma_0^x + \gamma_x^x x + \gamma_y^x y + \gamma_z^x z \tag{6}$$

Control points (sometimes named domain element points) are used here to decouple the shape parameters from the surface mesh, and provide a flexible framework through which to control the shape of a base geometry. Setting up a global RBF volume interpolation for n_c control points then requires a solution to a linear system, see[6] for more details, to ensure exact recovery of the control point data, in this case deformations:

$$\Delta\mathbf{x}^c = \mathbf{C}\boldsymbol{\alpha}^x \tag{7}$$
$$\Delta\mathbf{y}^c = \mathbf{C}\boldsymbol{\alpha}^y \tag{8}$$
$$\Delta\mathbf{z}^c = \mathbf{C}\boldsymbol{\alpha}^z \tag{9}$$

Polynomials are not included here, due to their growing radial influence, and so (superscript c represents a control point):

$$\Delta\mathbf{x}^c = \begin{pmatrix} \Delta x_1^c \\ \vdots \\ \Delta x_{n_c}^c \end{pmatrix}, \quad \boldsymbol{\alpha}^x = \begin{pmatrix} \alpha_1^x \\ \vdots \\ \alpha_{n_c}^x \end{pmatrix} \tag{10}$$

(analogous definitions hold for y and z coordinates) and the control point dependence matrix, $\mathbf{C}$, takes the form

$$\mathbf{C} = \begin{pmatrix} \phi_{11} & \cdots & \phi_{1n_c} \\ \vdots & \ddots & \vdots \\ \phi_{n_c1} & \cdots & \phi_{n_cn_c} \end{pmatrix} \tag{11}$$

where

$$\phi_{ij} = \phi(\|\mathbf{x}_i^c - \mathbf{x}_j^c\|) \tag{12}$$

For surface and volume mesh deformation, it is sensible to use decaying basis functions, to give the interpolation a local character and ensure deformation is contained in a region near the moving body, and Wendland's C^2 function[43] is used here. It is also sensible to not include polynomial terms, since these will transfer deformation throughout the entire mesh.

Hence, in the case considered here the global influence on any point in the aerodynamic mesh (denoted by superscript a) from the control points is determined by equation 4, which is applied as

$$\Delta x^a = \sum_{i=1}^{n_c} \alpha_i^x \phi(\|\mathbf{x}^a - \mathbf{x}_i^c\|) \tag{13}$$
$$\Delta y^a = \sum_{i=1}^{n_c} \alpha_i^y \phi(\|\mathbf{x}^a - \mathbf{x}_i^c\|) \tag{14}$$
$$\Delta z^a = \sum_{i=1}^{n_c} \alpha_i^z \phi(\|\mathbf{x}^a - \mathbf{x}_i^c\|) \tag{15}$$

Hence, the design variables are the modal deformations, which give control point perturbations, which hence are decoupled from the surface and volume meshes.

II.C. Control Point Deformations

The method for deriving surface design parameters and the methods for perturbing the CFD mesh have been presented. The derived parameters are, however, surface deformations but for the aerodynamic optimization process, control point parameters are required. Previous work has involved placing control points away from the surface, to form off-surface domain elements, and this has proven very effective, and is used again for the optimization case later. In two dimensions, the control points to define the modal deformations are located on the surface of the aerofoil section. This ensures that there is direct coupling between the control point deformations and the surface deformations that derived them.

The deformation modes derived by SVD, are extracted from a training library of aerofoils, and the control points, 24 are used here, are independent of a base geometry. A 'shrink-wrapping' method is used to map them onto the geometry being considered. Figure 2 shows the surface control points and an example deformation of a single control point for a NACA0012 mesh.

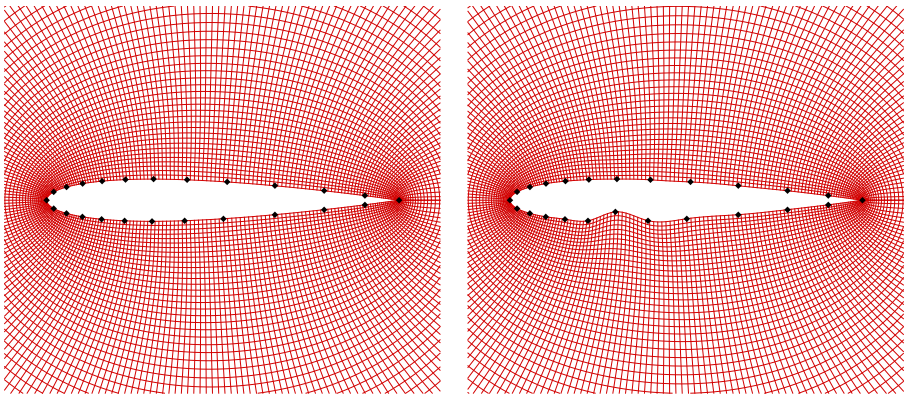

(a) Control points (b) Example deformation

Figure 2: Surface-based control points and example deformation.

II.D. Computation of Deformation Field

The modal deformations can be applied to any geometry, and are extracted using a training library wherein all aerofoils have been normalised to unit chord and all have leading and trailing edges at $z(0) = z(1) = 0$. Hence, each mode is rotated to the local aerofoil axis system. In three dimensions, a set of n_s sectional slices of control points are applied to the surface at regular intervals. However, when these are deformed, the variation of the deformation field between the sections can either be defined explicitly or left to the global interpolation field. The latter is normally used, but this means that interpolation properties, for example basis function chosen and support radius set, will influence the deformed surface. That effect is undesirable, so is eliminated here, as it can result in a more global influence of an effectively local deformation. Intermediate sections are defined between each deformed slice, and the deformation of these is controlled. The spanwise region between each section is split into n_i intermediate regions, and so the total number of sections becomes $1 + (n_s - 1)n_i$.

The geometry considered here is the MDO wing[45, 46, 47] (see later). The surface is preprocessed to compute the local chord length at each section, and the initial rotation angle of each section. The control point sections are then applied to the surface by scaling by local chord, rotating by local incidence, and shrink-wrapping to the exact geometry using a local geometric intersection algorithm. Figure 3 shows the control points resulting from using $n_s = 10$ and $n_i = 4$, for the surface mesh used later. This means there are 37 control point sections but only 10 are deformed by the design parameters. The deformed points are shown in green, and the controlled points in black.

Consider first the deformation field for global application of the modal parameters. In this case the modal deformations are applied using a single global weighting, i.e. one design variable for each mode, with local effects due only to scaling the modal deformations by local chord and rotating by local section incidence. For local deformations, i.e. one design variable for each mode at each of the n_s sections, a basis function can

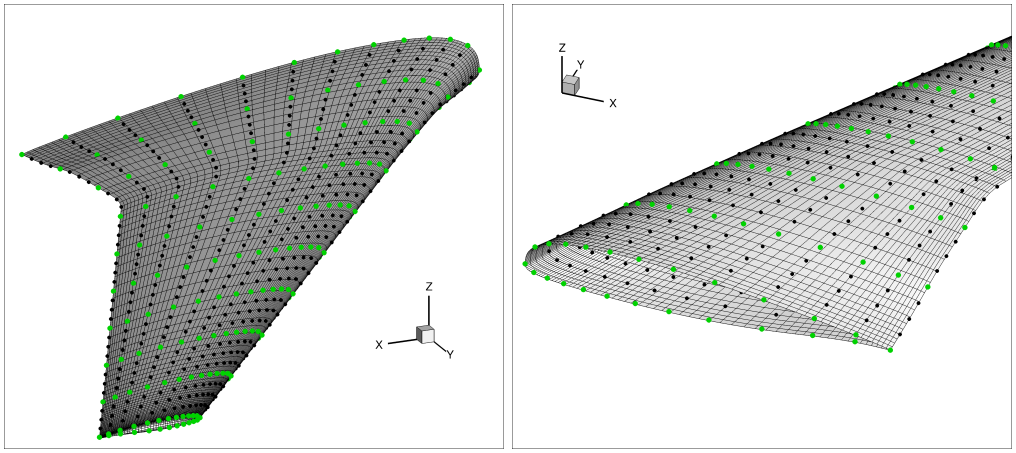

Figure 3: Surface mesh and control points.

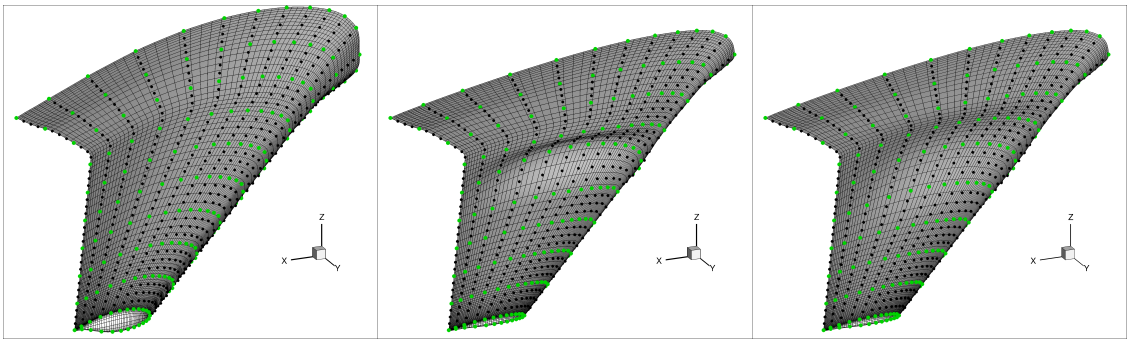

(a) Mode 1 global (b) Mode 1 local, width 1 (c) Mode 1 local, width 2

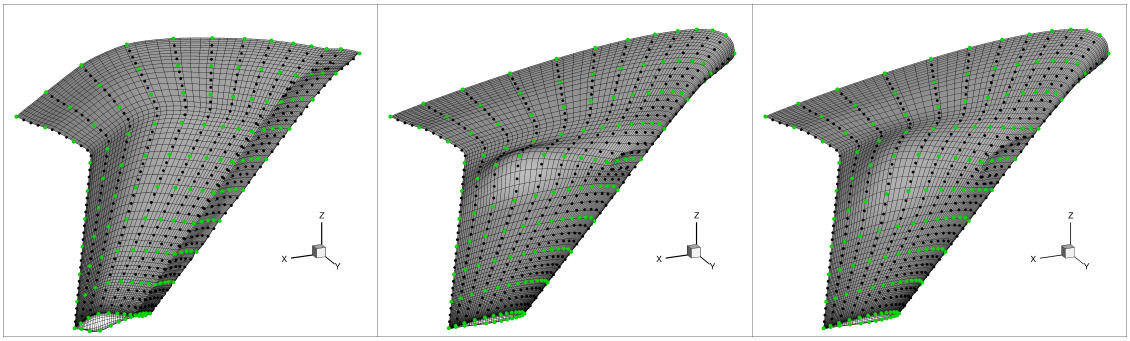

(d) Mode 3 global (e) Mode 3 global, width 1 (f) Mode 3 global, width 2

Figure 4: Surface and control point modal deformations. Mode 1 and mode 3.

be used to determine how the deformation of each of the n_s sections affects the other sections, i.e. controls the zone of influence. This can be left to the global interpolation, but is defined here to allow control of the decay. A width variable, n_w, is defined to determine the deformation decay from each section, and this defines over how many sections the effect decays to zero. A basis function is then defined such that for a width of one, i.e. the effect of the sectional deformation decays to zero at the neighbouring sections each side, a global modal deformation can be recovered exactly.

Figure 4 shows the control point locations and resulting surface mesh for deformations using the first and third modes; left column shows a global modal deformation, and centre and right columns local modal deformations of the fifth control point section using $n_w = 1$ and $n_w = 2$. The modal deformation magnitude is exaggarated to 10% local chord for illustration purposes. This improved localisation process is also adopted to improve the application of off-surface domain element perturbations, used previously by the authors.

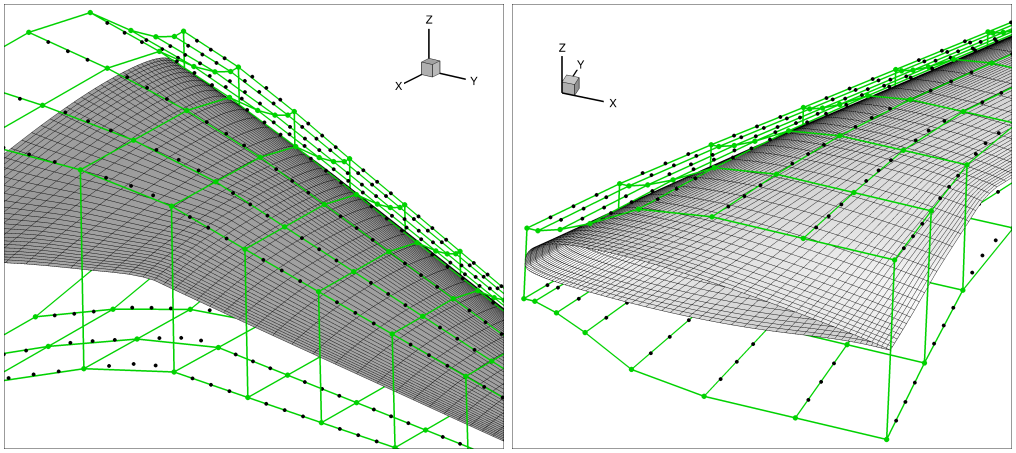

Figure 5: Surface mesh and off-surface control points.

III. Optimization Approach

Typically, the two main types of numerical optimization algorithm that are chosen for aerodynamic optimization are gradient-based and global search. Gradient-based methods, such as conjugate gradient and sequential quadratic programming (SQP) use the local gradient as a basis from which to construct a search direction. The algorithm starts at an initial solution and marches in a direction towards to minimum solution. Global search methods, however, use a number of agents with different starting positions within the search space. These agents then cooperate and move by various, often nature inspired, mechanisms towards the global optimum solution.

The suitable selection of a gradient-based or a global search algorithm to perform aerodynamic optimization is highly dependent on the optimization case analysed, specifically the degree of modality present in the situation. Multimodal problems are characterised by multiple local optima, where one or more of those local optima is the globally optimum solution. This can be particularly problematic for gradient-based optimizers due to premature convergence in a local minimum that is not necessarily close to the global optimum. Agent-based methods can alleviate this issue somewhat. Within the context of aerodynamic shape optimization, the presence of a multimodal search space is highly dependent on the extent of the surface representation and the fidelity of the flow analysis tool. The issue of degree of multimodality in aerodynamic optimization problems is an unanswered question, with work presented showing that multimodality exists in a number of cases, but unimodal cases also exist.[48,49,50,11] Chernukhin and Zingg[11] have considered this issue by testing a number of different optimization problems and shown that for a b-spline parameterization of the surface, viscous, compressible drag minimization of the RAE2822 aerofoil has one global optimum. They also showed multiple local optima for other problems.

III.A. Feasible Sequential Quadratic Programming (FSQP)

The feasible sequential quadratic programming (FSQP)[51,52] algorithm is used here, and is an efficient constrained local gradient-based optimization algorithm. FSQP approximates the Lagrangian of the optimization problem by a quadratic programming (QP) subproblem, such that a solution to this can be found which is the step direction of the algorithm. The QP subproblem at every major timestep is given as an active set problem:

$$\begin{aligned} \underset{\Delta\boldsymbol{\beta}\in\Re^n}{\text{minimise}} \quad & \frac{1}{2}\Delta\boldsymbol{\beta}^T\mathbf{H}\Delta\boldsymbol{\beta} + \nabla J(\boldsymbol{\beta})^T\Delta\boldsymbol{\beta} \\ \text{subject to} \quad & \nabla g_i(\boldsymbol{\beta})^T\Delta\boldsymbol{\beta} + g_i(\boldsymbol{\beta}) \leq 0 \quad i \in v \end{aligned} \tag{16}$$

where J is the objective function, $\boldsymbol{\beta}$ is the design vector, g are the equality and inequality constraints, and v represents the integers of the constraints that are active. The solution to this problem is a minimum of the approximated quadratic and therefore gives the direction along which to search. This solution requires the Hessian, or an approximation to the Hessian at every major timestep, which in turn requires sensitivity

of the objective function and constraints with respect to the design variables. Here these are obtained by a second-order central-difference scheme, so the number of objective function evaluations is proportional to the number of design variables. It is more computationally efficient to create an approximation to the Hessian instead of calculating the Hessian at every major timestep, so the Hessian is updated using a suitable quasi-Newton method to ensure a positive definite Hessian and therefore ensure a decreasing objective function. The algorithm evolves until the Kuhn-Tucker conditions are satisfied, which then represent a converged solution using a constrained gradient-based optimizer. The line search is a non-monotone procedure[53] that results in a decrease in the objective function within at most four iterations, meaning that an increase in the objective function can also result within those four iterations.

For computational efficiency, the sensitivity evaluation has been parallelised based on the number of design variables such that the evaluation of the sensitivity of the objective function and constraints with respect to the design variables is split between the number of CPUs available.[6,7] This is necessary as, within the ASO environment, an objective function evaluation represents a CFD solution, so this formulation allows parallel evaluation of the required sensitivities. Constraint and step-size evaluations and optimizer updates occur on the master process, and each CPU controls the geometry (and CFD volume mesh) perturbations corresponding to the different design variables, and calls the flow solver. Flow-solver results are then returned to the master for optimizer updates.

III.B. Flow Solver

The flow-solver used is a structured multiblock finite-volume code, with upwind spatial discretisation, using the flux vector splitting of van Leer,[54] and multi-stage Runge-Kutta time-stepping. Convergence acceleration is achieved through multigrid.[55]

IV. Application of Modal Design Variables in Three Dimensions

IV.A. Problem Definition

Optimization is applied here to the MDO wing (a large modern transport aircraft wing, the result of a previous Brite-Euram project[45,46,47]) in the economical transonic cruise condition, defined by Allwright[45,46,47] as Mach 0.85 with the wing trimmed to obtain a lift coefficient of 0.452. This design case is well suited to inviscid flow analysis, since induced and wave drag are dominant here. Compressible transonic wing optimization for drag minimization subject to strict constraints is investigated, and so the problem definition is:

Objective:	Minimize drag (C_D)
Constraint 1 (lift):	$C_L \geq C_L^0$
Constraint 2 (moment):	$C_{Mx} \leq C_{Mx}^0$
Constraint 3 (moment):	$C_{My} \leq C_{My}^0$
Constraint 4 (internal volume):	$V \geq V^0$

A 688,000 cell, block-structured C-H mesh was generated;[56] 129×81 surface mesh, 33 points on either side of the wake, 33 points in the tip-slit, and 33 points between inner and outer boundary. Figure 6 shows domain, boundaries and farfield mesh, and Figure 7 two views of the surface mesh and chordwise planes.

In previous work the authors have applied a 16-point off-surface domain element for an aerofoil, and a set of section-based domain elements for a wing, which has been shown to be very effective.[6,7] Hence, an improved version of this approach is used here as a comparison with the new method; the 24-point on-surface set of control points used in two dimensions is again used here. The same evenly-distributed set of slices is used as above, but the points at each slice are 'shrink-wrapped' to the local surface. Figure 5 shows two views of the located control point spanwise locations.

Four optimizations of the MDO wing were run using different design variables, all with the parallel FQSP optimizer. The drag comprises pressure, induced, and wave drag components, and it is most efficient to address these separately. Hence, the induced drag is considered by first running a twist only optimization, and optimizations to minimize the remaining drag restarted from this geometry.

1. Twist case. To address the induced drag effect, a simple case was first run using a global linear twist variable, plus a global pitch variable to allow load balancing. This results in two variables.

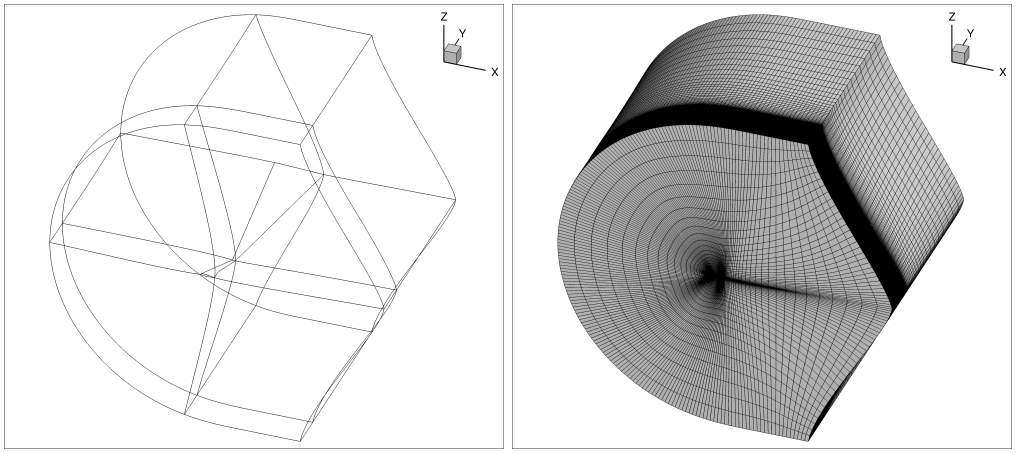

Figure 6: Domain and block boundaries and farfield mesh.

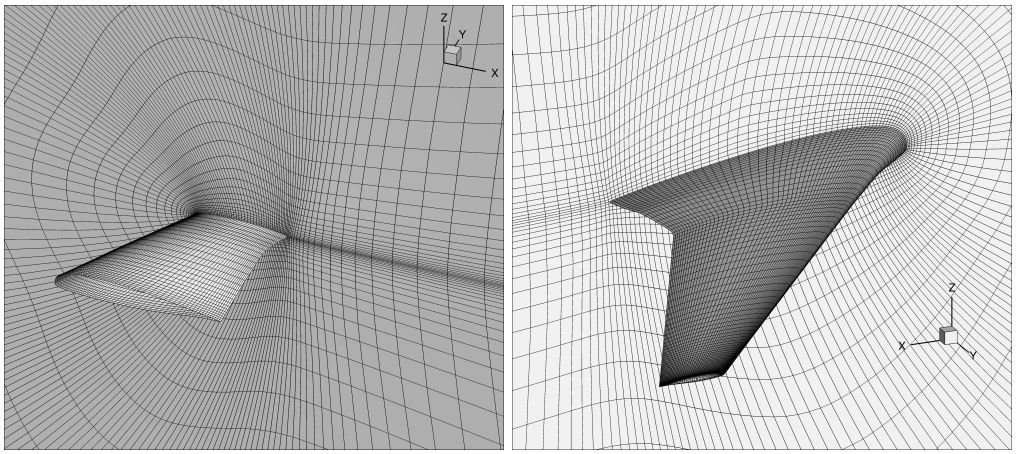

Figure 7: Surface mesh and selected mesh planes.

2. Individual point deformation case. Conventional off-surface domain element, with individual deformations of each point in each of the 10 slices, plus a global linear twist variable and a global pitch variable to allow load balancing. This results in $10 \times 16 + 2 = 162$ variables.

3. Global mode case. Global modal deformations of all 10 sectional slices using six modes, a global linear twist variable, plus a global pitch variable to allow load balancing. This results in $6+2 = 8$ variables. A global mode is a single deformation of all control points, with the modes scaled and rotated according to the local geometry.

4. Local mode case. Local modal deformation using six modes at each of the 10 sectional locations, a global linear twist variable, plus a global pitch variable to allow load balancing. This results in $10 \times 6 + 2 = 62$ variables. In all cases $n_w = 1$. Again at each section, the local modes are scaled and rotated according to the local geometry. Global modes are not included too, since these can be recovered exactly from combinations of the local modes.

IV.B. Results

Table 1 presents results of the four sets of variables. The twist variables are clearly effective at reducing the induced drag, and the finer surface deformations then reduce the pressure and wave drag. Figure 8 shows the upper surface pressure contours for the baseline case, the optimization using 16-point domain element deformations at each section, six global modes, and six local modes. Sectional pressure coefficient variations are also presented in figure 9. Hence, the local mode case has produced a shock-free solution.

Table 1: Optimization results (C_D in counts)

Variables	Parameters	C_L	C_D	ΔC_D	Evolutions	CFD calls
Baseline Geometry		0.452	153.8	-	-	-
Twist	2	0.452	142.2	**-7.5%**	20	111
Domain Element	162	0.452	108.6	**-29.4%**	114 (+20)	37502
Modes: 6 Global	8	0.452	112.7	**-26.7%**	41 (+20)	827
Modes: 6 Local	62	0.452	106.9	**-30.5%**	75 (+20)	9887

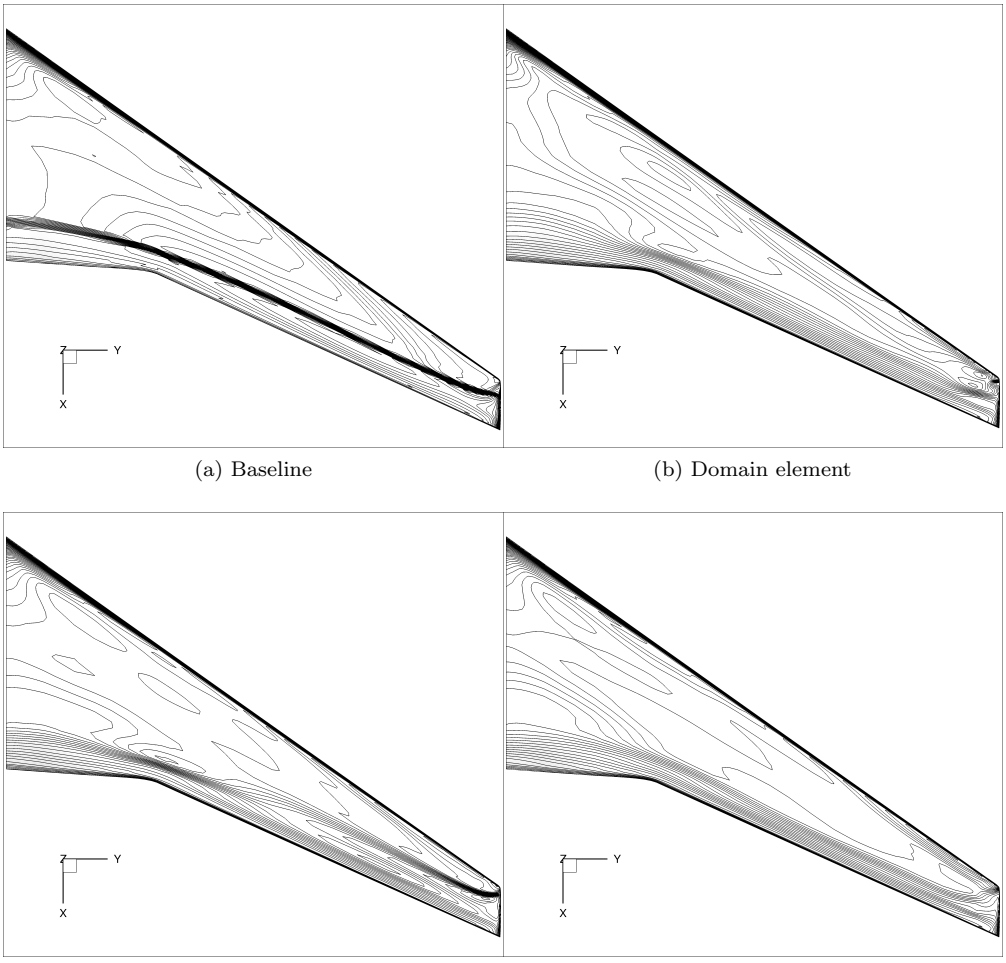

(a) Baseline (b) Domain element

(c) Modes 6 global (d) Modes 6 local

Figure 8: Upper surface pressure coefficient: Initial, domain element, 6 global modes, 6 local modes.

The convergence histories, in terms of evolutions and function evaluations are shown in figure 10. Table 1 also includes the number of objective evaluations (flow solutions) required. The optimizer adopts a second-order central finite-difference gradient evaluation, and so each evolution requires two flow solutions per variable, and a further one or two solutions for the step size evaluation. Hence, the global modes are particularly efficient, requiring 45× fewer evaluations than the off-surface domain element, for similar drag reduction. However, neither of these approaches has eliminated the wave drag entirely, whereas the local modes have achieved this for significantly lower cost than the domain element approach.

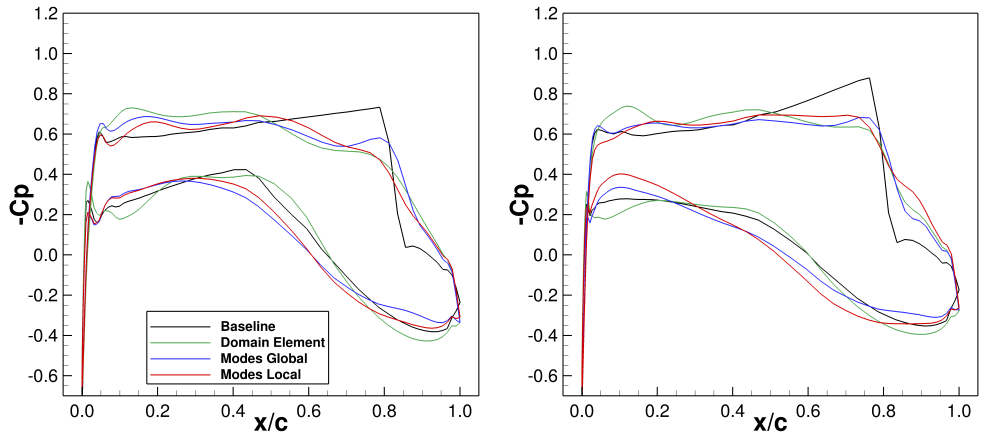

(a) y/s = 0.2 (b) y/s = 0.4

(c) y/s = 0.6 (d) y/s = 0.8

Figure 9: Sectional pressure coefficient. y/s = 0.2, 0.4, 0.6, 0.8.

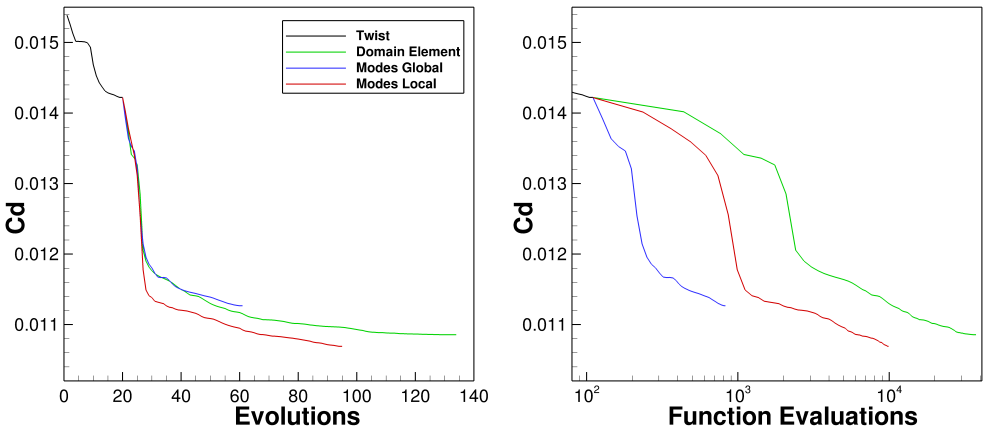

Figure 10: Convergence histories.

V. Conclusions

Aerodynamic shape optimization has been considered, using mathematically-derived design variables. Orthogonal design variables have been extracted by a singular value decomposition approach where a training

library of aerofoils is analysed and decomposed to obtain an efficient and reduced set of design variables; these are geometric 'modes' of the original library, representing typical aerofoil design parameters. In the aerodynamic shape optimization framework a surface and mesh deformation algorithm is required, and a control point approach has been adopted. This adopts a small number of control points which are linked to the numerical mesh points by a global volume interpolation using radial basis functions to allow large, smooth deformations of the mesh.

The performance of the mathematical design variables has been demonstrated in three dimensions, with results of optimization of the MDO wing in transonic flow. The modal deformations have been applied as both local and global variables, and a further case run with a previously-used off-surface domain element approach. An effective geometric application method has also been developed, allowing improved local control of deformations, and exact recovery of global modes from local modes. It has been demonstrated that the modal approach gives better results than the domain element approach, for significantly fewer design variables and, furthermore, using global modes alone, an impressive result is achieved with only eight variables.

References

[1]R. M. Hicks and P. A. Henne. Wing design by numerical optimization. *Journal of Aircraft*, 15(7):407–412, 1978.

[2]N. Qin, A. Vavalle, A. Le Moigne, M. Laban, K. Hackett, and P. Weinerfelt. Aerodynamic considerations of blended wing body aircraft. *Progress in Aerospace Sciences*, 40(6):321–343, 2004.

[3]E. J. Nielsen, E. M. Lee-Rausch, and W. T. Jones. Adjoint based design of rotors in a noninertial frame. *Journal of Aircraft*, 47(2):638–646, 2010.

[4]Z. Lyu, G. K. W. Kenway, and J. R. R. A. Martins. Aerodynamic shape optimization investigations of the common research model wing benchmark. *AIAA Journal*, 53(4):968–985, 2015.

[5]S. Choi, K. H. Lee, M. Potsdam, and J. J. Alonso. Helicopter rotor design using a time–spectral and adjoint based method. *Journal of Aircraft*, 51(2):412–423, 2014.

[6]A. M. Morris, C. B. Allen, and T. C. S. Rendall. CFD–based optimization of aerofoils using radial basis functions for domain element parameterization and mesh deformation. *International Journal for Numerical Methods in Fluids*, 58(8):827–860, 2008.

[7]A. M. Morris, C. B. Allen, and T. C. S. Rendall. Domain–element method for aerodynamic shape optimization applied to a modern transport wing. *AIAA Journal*, 47(7):1647–1659, 2009.

[8]C. B. Allen and T. C. S. Rendall. Computational-fluid-dynamics-based optimisation of hovering rotors using radial basis functions for shape parameterisation and mesh deformation. *Optimization and Engineering*, 14:97–118, 2013.

[9]M. Imiela. High-fidelity optimization framework for helicopter rotors. *Aerospace Science and Technology*, 23:2–16, 2012.

[10]J. E. Hicken and D. W. Zingg. Aerodynamic optimization algorithm with integrated geometry parameterization and mesh movement. *AIAA Journal*, 48(2):400–413, 2010.

[11]O. Chernukhin and D. W. Zingg. Multimodality and global optimization in aerodynamic design. *AIAA Journal*, 51(6):1342–1354, 2013.

[12]A. Jahangirian and A. Shahrokhi. Aerodynamic shape optimization using efficient evolutionary algorithms and unstructured CFD solver. *Computers and Fluids*, 46:270–276, 2011.

[13]L. Blasi and G. Del Core. Particle swarm approach for finding optimum aircraft configuration. *Journal of Aircraft*, 44(2):679–682, 2007.

[14]P. Castonguay and S. K. Nadarajah. Effect of shape parameterization on aerodynamic shape optimization. In *45th AIAA Aerospace Sciences Meeting and Exhibit*, Reno, Nevada, 2007. AIAA Paper 2007–59.

[15]D. J. Poole, C. B. Allen, and T. C. S. Rendall. Metric-based mathematical derivation of efficient airfoil design variables. *AIAA Journal*, 53(5):1349–1361, 2015.

[16]D. A. Masters, N. J. Taylor, T. C. S. Rendall, C. B. Allen, and D. J. Poole. Review of aerofoil parameterisation methods for aerodynamic shape optimisation. In *53rd AIAA Aerospace Sciences Meeting*, Kissimmee, Florida, 2015. AIAA Paper 2015–0761.

[17]J. A. Samareh. Survey of shape parameterization techniques for high fidelity multidisciplinary shape optimization. *AIAA Journal*, 39(5):877–884, 2001.

[18]A. Mousavi, P Castonguay, and S. K. Nadarajah. Survey of shape parameterization techniques and its effect on three dimensional aerodynamic shape optimization. In *18th AIAA Computational Fluid Dynamics Conference*, Miami, Florida, 2007. AIAA Paper 2007–3837.

[19]B. M. Kulfan. Universal parametric geometry representation method. *Journal of Aircraft*, 45(1):142–158, 2008.

[20]H. Sobieczky. Parametric airfoils and wings. *Notes on Numerical Fluid Mechanics*, 68:71–88, 1998.

[21]M. I. G. Bloor and M. J. Wilson. Generating parameterizations of wing geometries using partial differential equations. *Computer Methods in Applied Mechanics and Engineering*, 148:125–138, 1997.

[22]V. Braibant and C. Fleury. Shape optimal design using B–splines. *Computer Methods in Applied Mechanics and Engineering*, 44(3):247–267, 1984.

[23]F. Zhu and N. Qin. Intuitive class/shape function parameterization for airfoils. *AIAA Journal*, 52(1):17–25, 2014.

[24]A. Jameson. Aerodynamic design via control theory. *Journal of Scientific Computing*, 3(3):233–260, 1988.

[25]J. A. Samareh. Novel multidisciplinary shape parameterization approach. *Journal of Aircraft*, 38(6):1015–1024, 2001.

[26]W. Yamazaki, S. Mouton, and G. Carrier. Geometry parameterization and computational mesh deformation by physics-based direct manipulation approaches. *AIAA Journal*, 48(8):1817–1832, 2010.

[27]D. J. Poole, C. B. Allen, and T. C. S. Rendall. Control point-based aerodynamic shape optimization applied to aiaa adodg test cases. In *53rd AIAA Aerospace Sciences Meeting*, Kissimmee, Florida, 2015. AIAA Paper 2015–1947.

[28]D. J. Poole, C. B. Allen, and T. C. S. Rendall. Aerofoil inviscid drag minimization by constrained global optimization. In *11th World Congress on Computational Mechanics*, Barcelona, Spain, 2014.

[29]J. Reuther, A. Jameson, J. Farmer, L. Martinelli, and D. Saunders. Aerodynamic shape optimization of complex aircraft configurations via an adjoint formulation. In *34th AIAA Aerospace Sciences Meeting and Exhibit*, Reno, Nevada, 1996. AIAA Paper 1996–94.

[30]A Jameson, N. A. Pierce, and L. Martinelli. Optimum aerodynamic design using the navier–stokes equations. In *35th AIAA Aerospace Sciences Meeting and Exhibit*, Reno, Nevada, 1997. AIAA Paper 1997–101.

[31]A. Jameson. CFD for aerodynamic design and optimization: its evolution over the last three decades. In *16th AIAA Computational Fluid Dynamics Conference*, Orlando, Florida, 2003. AIAA Paper 2003–3438.

[32]T. M. Leung and D. W. Zingg. Aerodynamic shape optimization of wings using a parallel newton-krylov approach. *AIAA Journal*, 50(3):540–550, 2012.

[33]H Gagnon and D. W. Zingg. Two-level free-form deformation for high-fidelity aerodynamic shape optimization. In *12th AIAA Aviation Technology, Integration and Operations (ATIO) Conference and 14th AIAA/ISSMO Multidisciplinary Analysis Optimization Conference*, Indianapolis, Indiana, 2012. AIAA Paper 2012–5447.

[34]C. A. Mader and J. R. R. A. Martins. Stability-constrained aerodynamic shape optimization of flying wings. *Journal of Aircraft*, 50(5):1431–1449, 2013.

[35]Z. Lyu and J. R. R. A. Martins. Aerodynamic shape optimization studies of a blended-wing-body aircraft. *Journal of Aircraft*, 51(5):1604–1617, 2014.

[36]B. Epstein and S. Peigin. Optimization of 3D wings based on navier-stokes solutions and genetic algorithms. *International Journal of Computational Fluid Dynamics*, 20(2):75–92, 2006.

[37]D. J. Poole, C. B. Allen, and T. C. S. Rendall. Comparison of local and global constrained aerodynamic shape optimization. In *32nd AIAA Applied Aerodynamics Conference*, Atlanta, Georgia, 2014. AIAA Paper 2014–3223.

[38]I. C. Chang, F. J. Torres, and C. Tung. Geometric analysis of wing sections. Technical report, NASA Ames Research Centre, Moffett Field, California, April 1995. NASA Technical Memorandum 110346.

[39]G. M. Robinson and A. J. Keane. Concise orthogonal representation of supercritical airfoils. *Journal of Aircraft*, 38(3):580–583, 2001.

[40]D. J. J. Toal, N. W. Bressloff, A. J. Keane, and C. M. E. Holden. Geometric filtration using proper orthogonal decomposition for aerodynamic design optimization. *AIAA Journal*, 48(5):916–928, 2010.

[41]S. S. Ghoman, Z. Wang, P. C. Chen, and R. K. Kapania. A POD-based reduced order design scheme for shape optimization of air vehicles. In *53rd AIAA/ASME/ASCE/AHS/ASC Structures, Structural Dynamics and Materials Conference and Co-located Events*, Honolulu, Hawaii, 2012. AIAA Paper 2012–1808.

[42]M. Buhmann. *Radial Basis Functions*. Cambridge University Press, 1st edition, 2005.

[43]H. Wendland. *Scattered Data Approximation*. Cambridge University Press, 1st edition, 2005.

[44]T. C. S. Rendall and C. B. Allen. Unified fluid–structure interpolation and mesh motion using radial basis functions. *International Journal for Numerical Methods in Engineering*, 74(10):1519–1559, 2008.

[45]S. Allwright. Multi-discipline optimisation in preliminary design of commercial transport aircraft. In *Computational Methods in Applied Sciences '96 (ECCOMAS)*, pages 523–526, Paris, France, 1996. Wiley, New York.

[46]S. Allwright. Multi-discipline optimisation in preliminary design of commercial transport aircraft. *Computational Methods in Applied Sciences, ECCOMAS*, pages 523–526, 1996.

[47]D. Haase, V. Selmin, and B. Winzell. *Progress in Computational Flow-Structure Interaction*. Springer, New York, 2002.

[48]H. Namgoong, W. Crossley, and A. S. Lyrintzis. Global optimization issues for transonic airfoil design. In *9th AIAA/ISSMO Symposium on Multidisciplinary Analysis and Optimization*, Atlanta, Georgia, 2002. AIAA Paper 2002–5641.

[49]M. S. Khurana, H. Winarto, and A. K. Sinha. Airfoil optimisation by swarm algorithm with mutation and artificial neural networks. In *47th AIAA Aerospace Sciences Meeting Including the New Horizons Forum and Aerospace Exposition*, Orlando, Florida, 2010. AIAA Paper 2009–1278.

[50]H. P. Buckley, B. Y. Zhou, and D. W. Zingg. Airfoil optimization using practical aerodynamic design requirements. *Journal of Aircraft*, 47(5):1707–1719, 2010.

[51]E. Panier and A. L. Tits. On combining feasibility, descent and superlinear convergence in inequality constrained optimization. *Mathematical Programming*, 59:261–276, 1993.

[52]J. L. Zhou, A. L. Tits, and C. T. Lawrence. Users guide for FSQP version 3.7 : A fortran code for solving optimization programs, possibly minimax, with general inequality constraints and linear equality constraints, generating feasible iterates. Technical report, Institute for Systems Research, University of Maryland, 1997. SRC-TR-92-107r5.

[53]J. L. Zhou and A. L. Tits. Nonmonotone line search for minimax problems. *Journal of Optimization Theory and Applications*, 76(3):455–476, 1993.

[54]I. H. Parpia. Van-leer flux vector splitting in moving coordinates. *AIAA Journal*, 26:113–115, 1988.

[55]C. B. Allen. Multigrid convergence of inviscid fixed- and rotary-wing flows. *International Journal for Numerical Methods in Fluids*, 39(2):121–140, 2002.

[56]C. B. Allen. Towards automatic structured multiblock mesh generation using improved transfinite interpolation. *International Journal for Numerical Methods in Engineering*, 74(5):697–733, 2008.